

Study and Optimization of High-Bit Rate Optical Fiber Transmission

Mimouna Oukli¹, Malika Kandouci¹,
Meriem Bouzid¹, Abdelber Bendaoud²

Abstract: In this article, we present the modelling of an optical communication link using the optical standard single-mode fiber working at $\lambda = 1.55\mu\text{m}$ single wavelength. The simulation confirmed the experimental characteristics like the photodetector sensibility, bit error rate (BER), the eye pattern, as well as the limitations and the performance of such optical transmission system.

Keywords: Laser, Optical fiber, Optical amplification, Optical filter, Optical detection

1 Introduction

This paper presents a point-to-point optical link. Behavioural models for the electro optic conversion in transmitters (lasers) and receivers (detectors) and the propagation on single-mode fibers are presented as well. In addition, we will show that behavioural modelling allows the optimization of the parameters of physical components in terms of the bit error rate (BER).

2 Description of the Optical Link

We shall briefly present the models used to simulate a high-debit optical communication link, the analysis tools we have developed, and the optimization results. Fig. 1 shows the simulated link. The laser is directly modulated by a pseudorandom generator.

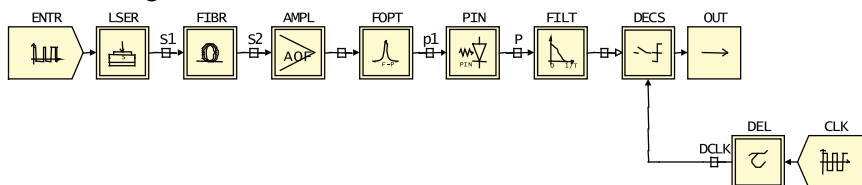


Fig. 1 – Optical communication link.

¹Laboratory of Signals and Systems Transmission, University of Sidi-Bel-Abbes, Algeria;
E-mail: mounaoukli@yahoo.fr

²Laboratory of Intelligent Control & Electrical Power Systems, University of Sidi-Bel-Abbes, Algeria;
E-mail: badelber@univ-sba.dz

The optical signal is transmitted along a standard single-mode fiber subsequent to the optical amplification and filtering detected by a photodiode. Post-processing tools allow us to draw the eye diagram, so as to automatically find the optimal decision threshold, as well as to extract the BER aimed at estimating the performance of the link.

3 Laser Model

The MQW DFB laser operates at $1.55\mu\text{m}$. It is directly modulated at 10 Gb/s using a non return-to-zero (NRZ) pseudorandom current signal. The current pulse from the laser driver is directly injected into coupled differential equations (1) which solve the electron–photon balance. The whole laser model has two coupled parts, i.e. a purely electrical one and the one describing the electro-optic behavior. Thus, it allows the inclusion of optronic components into a classical electronic CAD tool.

The electro-optic conversion is based on the rate equation approach: the behavior of a single-mode semiconductor laser above threshold is described by the following rate equations for the electron density $N(t)$:

$$\frac{dN(t)}{dt} = \frac{I}{eV} - \frac{n(t)}{\tau_s} - v_g g(t) S(t). \quad (1)$$

And the photon density $S(t)$ is [1]:

$$\frac{dS(t)}{dt} = \Gamma v_g g(t) S(t) - \frac{S(t)}{\tau_\phi} + \Gamma \beta \frac{N(t)}{\tau_s}. \quad (2)$$

The optical power and the complex envelope of electric field at the fiber input can then be expressed by:

$$P(t) = \frac{V\eta h\nu}{2\Gamma\tau_p} S(t), \quad (3)$$

$$E_{in}(t) = \sqrt{P(t)} e^{j\Phi}. \quad (4)$$

4 Fiber Model

The HDL-ATM fiber model includes only linear propagation phenomena (whereby the injected power remains weak, the Kerr effect may be neglected), so that the field at the fiber output E_{out} is computed as the convolution of its impulse response $h(t)$ and the input field $E_{in}(t)$:

$$E_{out}(t) = E_{in}(t) \otimes h(t) \quad (5)$$

and

$$P_{out}(t) = A |E_{in}(t) \otimes h(t)|^2, \quad (6)$$

with

$$h(t) = (1+j)(4\pi\beta_2 L)^{\frac{1}{2}} \exp(-jt^2/2\beta_2 L), \quad (7)$$

$A, L, D = 2\pi c\beta_2/\lambda_0^2$ stand for the attenuation, length and group velocity dispersion parameter of the fiber, respectively and $c, \beta_2,$ and λ_0 are the speed of light, the dispersion and the central wavelength of the optical signal, respectively.

In order to calculate E_{out} in the time domain, the infinite impulse response (IIR) $h(t)$ is approximated by a finite impulse response (FIR), numerical filter and a digital process block samples E_{in} which provides computing the convolution numerically.

$$E_{out}(KT_s) = \sum_{n=0}^{N-1} a(n) E_{in}(K-n)T_s, \quad (8)$$

where T_s represent the sampling period and N is the FIR filter order (RIF).

To obtain the filter coefficients $a(n)$, $h(t)$ is truncated and smoothed by the classical time window function $h_w(t)$.

$$h_w(t) = 0.54 + 0.46 \cos\left(\pi |t/NT_s|^p\right) \quad (9)$$

5 Detection

A. Principle of photo detection [7, 8]

The photons transmitted by fiber penetrate the detector made up of semiconductor material.

Being absorptive, photons can allow the electrons to pass for state of valence band in higher state of band conduction. Less dependent electrons become free. The photon thus leaves room to a pair electron-positron pair.

The potential difference is applied in order to prevent the electrons from falling down in its most stable state. Under the effect of the electric field, the two categories of carriers separate, and are involved towards zones where they are in a majority (named P or N). The carriers generated in such manner are then collected in the form of photocurrent. The number of electron-positron pairs is equal to the number of absorptive photons.

B. Characteristics of photo detection [7, 8]

Photons will not automatically undergo the photo detection. Firstly, a photon has to possess a superior or equal energy E_{photon} as high as the band of energy forbidden E_g to make cross the electron of the band of Valencia to the

band of conduction. It implies a cut wavelength λ_c beyond which the material becomes transparent in the brilliance. λ_c is determined by the energy of band forbidden E_g of the semiconductor according to the following relation:

$$E_{\text{photon}} = \frac{hc}{\lambda} \geq E_g \Rightarrow \lambda_c = \frac{hc}{E_g}. \quad (10)$$

The detector is supposed to be purely quadratic: the generated signal is proportional to the optical power output. The electrical signal is subsequently filtered. The decision circuit is modelled by an ideal sampler, in which the threshold and decision instants are adjustable.

6 Analysis Tools

The analysis tool developed in HDL-ATM computes quasi analytically the BER displaying the BER during the simulation.

In order to determine the BER, the simulation is first driven without any noise source, then each noise source is estimated and the variance of the global noise is finally expressed as:

$$\sigma^2 = \sigma_T^2 + \sigma_S^2 + \sigma_{sp-sp}^2 + \sigma_{sig-sp}^2 + \sigma_{S-sp}^2, \quad (11)$$

where σ_T^2 and σ_S^2 stand for variances of the thermal noise of electronic amplification circuit and the shot noise of photodiode, respectively. The other terms correspond to the beating of spontaneous emission of erbium-doped fiber amplifier (EDFA) with itself, the signal, and the shot noise. Analytical expressions for the terms appearing in (11) may be found in [2].

The BER is subsequently computed in a Gaussian approximation of the noise and exhibiting intersymbol interference like:

$$BER = \frac{1}{2M} \sum_{i=1}^M \operatorname{erfc} \left(\frac{|I_i - D|}{\sqrt{2\sigma_i}} \right) p(i), \quad (12)$$

Where M is the number of bits in the frame, D the decision threshold, I_i the mean value, σ_i the square mean value of intensity corresponding to symbol i and $p(i)$ the conditional probability of symbol i [3].

7 Results of Simulation

The figures that follow show the typical simulation results of a point-to-point link. In this example, the fiber impulse response has been approximated with $N = 100$ (see Section 3). The fiber model includes only linear propagation phenomena. The sampling criterion is largely satisfied since the sampling

frequency is 500 GHz being much higher than the laser signal bandwidth (10 GHz).

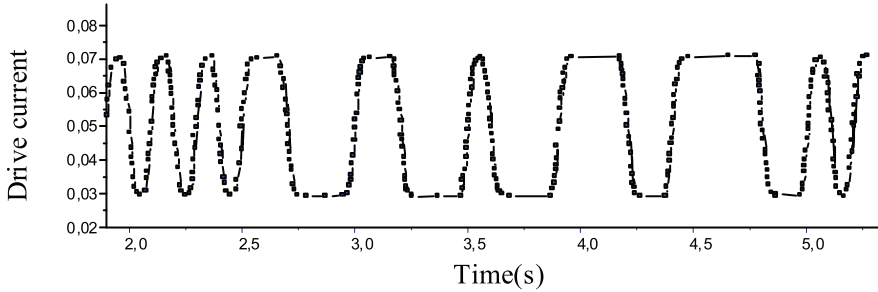


Fig. 2 – Drive current.

The Fig. 2 shows the current of modulation which serves for inciting the laser. One of the main advantages of the optical fiber laser for telecommunications is in the fact that it provides easy modulation: the modulation of the current which crosses it pulls directly the modulation of the emitted light either in intensity or in optical frequency.

The modelling of the interactions between the populations of photons and the bearers by the evolution equation allows us to explain a number of properties of this modulation.

The equations (13) and (14) are interpreted in the following manner: by unit of time, the density of bearers N , which disappears by spontaneous broadcast (spontaneous emission and the time of life of spontaneous emission), or by stimulated emission (term $g(t)s(t)$) including the injection of current I , (e is charge of electron, V – active volume, V/Γ – volume of mode, g – the earning and S is density of photon in the mode).

In the second equation, the density of photon in the whole of the mode occurs as the a result of stimulated emission (term $g(t)s(t)$) and of a fraction β of the spontaneous emission (term $\Gamma\beta n/\tau_s$) but disappears as a result of the internal losses α and the losses by mirrors α_m (τ_ϕ life span of the photons which includes these two terms of losses):

$$\frac{dN(t)}{dt} = \frac{I}{eV} - \frac{n(t)}{\tau_s} - v_g g(t)S(t), \quad (13)$$

$$\frac{dS(t)}{dt} = \Gamma v_g g(t)S(t) - \frac{S(t)}{\tau_\phi} + \Gamma\beta \frac{N(t)}{\tau_s}, \quad (14)$$

where v_g is the group velocity of guided wave light including the dispersion of the material. It is defined by the time of group.

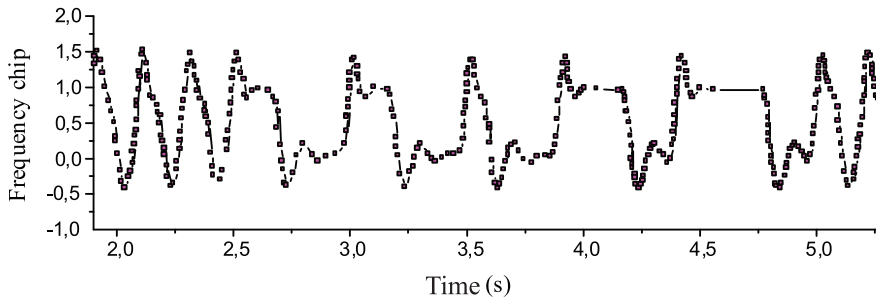


Fig. 3 – Frequency chip.

Fig. 3 represents the frequency chip which allows us to know the frequency at the moment given by the magnetic field.

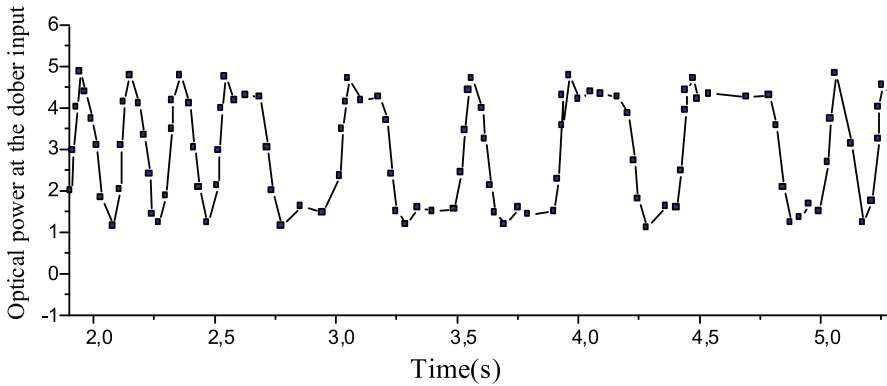


Fig. 4 – Optical power at the fiber input.

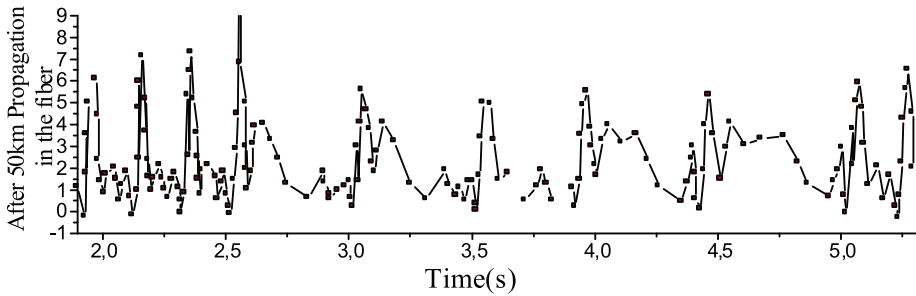


Fig. 5 – Optical power after 50km of propagation in the fiber.

Figs. 4 and 5 show respectively optical power at the fiber input and the one after 50km of propagation in the fiber. Therefore it is about the same signal, however the difference in optical power is observed, which is due to the enfeeblement (for the standard fiber the enfeeblement is esteemed by $A = 0.22\text{dB/km}$) of the signal which has been sodden by its propagating in the fiber.

The distortion of the signal can be observed, Fig. 5. Although being minimal in this kind of fiber, this distortion said standard fiber and with the wavelength $\lambda = 1.55\mu\text{m}$, it is not however unimportant, it is especially due to the dispersion.

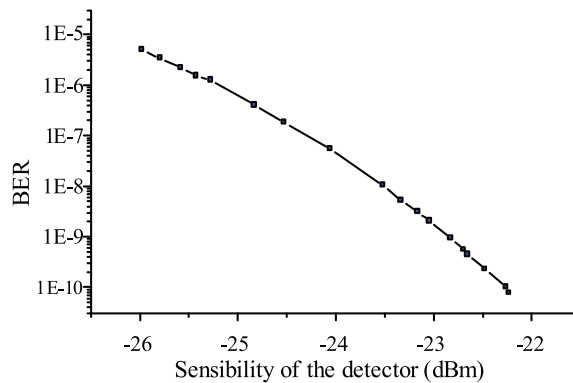


Fig. 6 – BER according to the sensibility of the detector (dBm).

The bit error rate provides measuring of the number of false bits. The rise in the optical power results in the increase in the report signal with noise. Hence the probability to see false bits in our transmission decreases.

Fig. 6 shows a curve of the BER according to sensibility of detector. We obtained a BER of 10^{-5} for the optical power of -26 dBm noticing that the BER decreases as the optical power increases, which justifies our earlier presumptions.

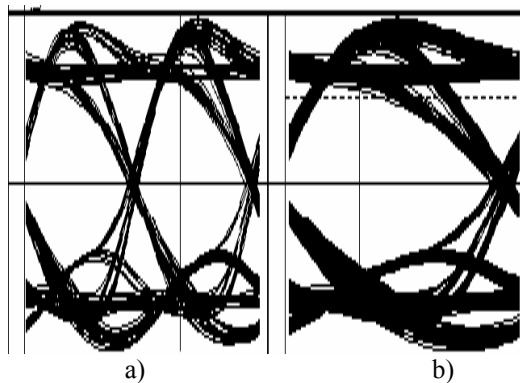


Fig. 7 – a) Noise parameters; b) Eye pattern.

Fig. 7 shows an eye pattern of electric signal detected in the borders of electric filter after amplification for current of 50 mA and for signal with $\lambda = 1.55 \mu\text{m}$ of wavelength. The injected power was 30 mA.

The degradation of the level "1" and the level "0" is obvious on Fig. 7, which is translated by a light lock of eye on vertical and horizontal plans.

The horizontal eye opening is induced by interference to intersymbol, which is essentially due the chromatic dispersal caused by the standard optical fiber, its dispersion coefficient being equal to $D = 16 \text{ps/nmkm}$.

The vertical eye opening is due to the occurrence of noise (thermic noise, amplification noise, noise of shot and that of photodiode), which is interpreted by blurred and widened tracks and degradation of error probability due to the intersymbol interference which is bigger as the eye is closed.

8 Mathematical Model

Taking into account coefficients of the sensibility of the detector as well as those of the BER (**Table 1**), we tried to establish a mathematical model by using "Regresionmod" software.

Table 1
Measured BER

Sensibility Detector (dBm)	TEB	Sensibility Detector (dBm)	TEB
-26	$4.84319 \cdot 10^{-6}$	-23.9956	$1.72247 \cdot 10^{-8}$
-25.9033	$3.80343 \cdot 10^{-6}$	-23.8462	$1.02034 \cdot 10^{-8}$
-25.6835	$2.34565 \cdot 10^{-6}$	-23.7055	$6.55129 \cdot 10^{-9}$
-25.5604	$1.76935 \cdot 10^{-6}$	-23.6264	$4.55924 \cdot 10^{-9}$
-25.4813	$1.33464 \cdot 10^{-6}$	-23.5648	$3.17291 \cdot 10^{-9}$
-25.411	$1.28195 \cdot 10^{-6}$	-23.4505	$1.95679 \cdot 10^{-9}$
-25.3758	$1.04811 \cdot 10^{-6}$	-23.3011	$1.25639 \cdot 10^{-9}$
-25.2879	$8.92149 \cdot 10^{-7}$	-23.2396	$1.02722 \cdot 10^{-9}$
-25.1209	$5.96362 \cdot 10^{-7}$	-23.1868	$8.06688 \cdot 10^{-10}$
-24.9187	$3.25926 \cdot 10^{-7}$	-23.0549	$4.2347 \cdot 10^{-10}$
-24.7868	$2.17867 \cdot 10^{-7}$	-22.9407	$2.83071 \cdot 10^{-10}$
-24.6462	$1.51621 \cdot 10^{-7}$	-22.8615	$2.05094 \cdot 10^{-10}$
-24.4967	$8.62701 \cdot 10^{-8}$	-22.7121	$9.93309 \cdot 10^{-11}$
-24.4264	$6.77491 \cdot 10^{-8}$	-22.6066	$5.88409 \cdot 10^{-11}$
-24.2593	$4.71487 \cdot 10^{-8}$	-22.5011	$3.62883 \cdot 10^{-11}$
-24.0835	$2.2835 \cdot 10^{-8}$		

Fig. 8 shows the comparison between simulated BER and measured BER.

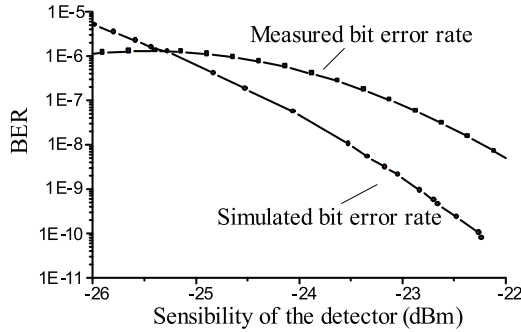


Fig. 8 – The comparison between simulated BER and measured BER.

The mathematical model that we established is a polynomial, and can be written as follows:

$$TEB = 2.60345093440033 \cdot 10^{-7} X + 1.12271020455085 \cdot 10^{-8} X^2.$$

9 Conclusion

The objective of this work was to estimate the advantages and the limits of a high debit optical link. For this purpose we used the simulator VHDL-AMS. Our transmission chain comprises a DFB laser, modulated directly by a pseudorandom generator whereby the optical signal is transmitted along a standard single-mode fiber on a single wavelength $\lambda = 1.55\mu\text{m}$, the chain of reception, which includes the optical amplifier (EDFA) instead of a repeater regenerator and optical filtering whereby the conversion of signal is made by means of one photodiode and electric filtering. The modules of the evaluation of the performances allow determining the eye pattern and the bit error rate (BER).

The results obtained by simulation suggest that the main limitation of such a transmission and the enfeeblement caused by the chromatic dispersal as well as the noise (accompanying the signal as it propagates and until its reception), which is interpreted by a distortion of the signal, is a decline and a loss in the optical power.

These limitations can be more important if we do not make the appropriate choice of each of the elements which constitute our optical link.

10 References

- [1] S. Mohrdiek, H. Burkhard, F. Steinhausen, H. Hillmer, R.Lösch, W. Schlapp, R. Göbel: 10-Gb/s Standard Fiber Transmission using Directly Modulated 1.55 μm Quantum-well DFB Laser, IEEE Photon. Technol. Lett., Vol. 7, No. 11, Nov. 1995, pp. 1357 – 1359.
- [2] G.P. Agrawal: Fiber-Optic Communication Systems, John Wiley & Sons, New York, 1992.

- [3] F.M. Gardner, J.D. Baker: *Simulation Techniques: Models of Communication Signals and Processes*, John Wiley & Sons, New York, 1997.
- [4] K. Vuorinen, F. Gaffiot, G. Jacquemod: *Modeling Single-mode Lasers and Standard Single-mode Fibers using a Hardware Description Language*, IEEE Photon. Technol. Lett., Vol. 9, No. 6, June 1997, pp 824 – 826.
- [5] Glavieux, M. Joindot: *Introduction aux communications numériques*, Collection Pédagogique de Télécommunication, Ellipses éditeur, 1991.
- [6] Jean-Louis Verneuil: *Simulation de systèmes de télécommunications par fibre optique à 40 Gbits/S*, Thèse de Doctorat Université de Limoges, 2003.
- [7] Erman Marko: *Tendances et évolution des réseaux et technologies optiques*, Revue des Télécommunications d'Alcatel, 3ème trimestre 2001, pp. 173 – 176.
- [8] Bruyere Frank: *Le multiplexage en longueur d'onde dans les réseaux métropolitains*, Revue des Télécommunications d'Alcatel, 1er trimestre 2002, pp. 27 – 32.